nature chemistry

ARTICLES

PUBLISHED ONLINE: 27 MARCH 2017 | DOI: 10.1038/NCHEM.2749

A polymer nanoparticle with engineered affinity for a vascular endothelial growth factor ($VEGF_{165}$)

Hiroyuki Koide[1,2], Keiichi Yoshimatsu[2], Yu Hoshino[3], Shih-Hui Lee[2], Ai Okajima[1], Saki Ariizumi[1], Yudai Narita[1], Yusuke Yonamine[2], Adam C. Weisman[2], Yuri Nishimura[3], Naoto Oku[1]*, Yoshiko Miura[3]* and Kenneth J. Shea[2]*

Protein affinity reagents are widely used in basic research, diagnostics and separations and for clinical applications, the most common of which are antibodies. However, they often suffer from high cost, and difficulties in their development, production and storage. Here we show that a synthetic polymer nanoparticle (NP) can be engineered to have many of the functions of a protein affinity reagent. Polymer NPs with nM affinity to a key vascular endothelial growth factor ($VEGF_{165}$) inhibit binding of the signalling protein to its receptor VEGFR-2, preventing receptor phosphorylation and downstream $VEGF_{165}$-dependent endothelial cell migration and invasion into the extracellular matrix. In addition, the NPs inhibit VEGF-mediated new blood vessel formation in Matrigel plugs *in vivo*. Importantly, the non-toxic NPs were not found to exhibit off-target activity. These results support the assertion that synthetic polymers offer a new paradigm in the search for abiotic protein affinity reagents by providing many of the functions of their protein counterparts.

Protein affinity reagents are widely used in basic research, industrial processes and clinical applications for isolation of individual proteins, for analytical or diagnostic purposes, and for their effect on biological systems by modulating the function of the target protein for mechanistic research or for therapeutic intervention. Antibodies or their fragments are the most common protein affinity reagents[1]. In addition, there are now a number of new technologies that are being developed to generate affinity reagents including antibody-like molecules that utilize novel protein scaffolds[2], oligomers (for example, RNA and DNA aptamers)[3], native or synthesized amino acid polypeptides[4], and various hybrids of these forms[5]. Despite the variety of approaches for generating biological affinity reagents, current limitations including time needed for their discovery, development and production, reagent cost, and robustness provide strong motivation to explore non-biological alternatives.

Affinity reagents such as antibodies and related biological macromolecules 'recognize' protein surfaces with combinations of 22 proteinogenic amino acids. The affinity is due to the sum total of complementary non-covalent interactions over surfaces that often exceed 1,500 $Å^2$ and involve at least 20–30 amino acid contacts from each partner. Unlike well-defined enzyme active sites that can be targeted by small organic molecules (that is, enzyme inhibitors), protein surfaces are mildly undulating and relatively featureless. An effective non-biological synthetic protein affinity reagent should engage a protein surface with multiple contacts over a substantial surface area, an attribute that challenges discovery of small organic molecular inhibitors of protein–protein complex formation[6].

Synthetic polymers have many features that make them attractive candidates as protein affinity reagents. They can be designed to be large and flexible, allowing them to map onto significant portions of a protein surface. In addition, they are relatively simple and inexpensive to produce and can be prepared rapidly on a large scale. As their synthesis does not require living organisms, biological contamination is avoided. Organic polymers are robust and can function under a variety of physiological and nonphysiological conditions. A broad range of chemical functionality is available to synthetic polymers permitting opportunities for affinity optimization. Furthermore, the size, physical properties and biomacromolecule affinity of many polymers can be influenced by external stimuli (temperature, pH, ionic strength) providing an extra dimension of control[7,8].

However, since synthetic polymers are prepared by a kinetically driven free radical polymerization, the sequence of functional monomers is not controlled. The absence of sequence control may be compensated to some degree by their conformational promiscuity. This would allow optimization of complementary interactions with protein surfaces by an induced fit, a process that finds many analogies in biology[9,10]. Compositional optimization permits 'focusing' on a particular biomacromolecule target by adjusting the chemical constituents of the nanoparticles (NPs). A lightly crosslinked network polymer presents 3D arrays of linear polymer segments that can serve as both continuous and discontinuous recognition elements for binding protein surfaces. Nevertheless, the advantages of synthetic polymers are tempered by the fact that the polymers are not pure substances, their affinity, for example, is the average of the ensemble of all the polymers in the measurement. In this regard, they may be viewed as primitive polyclonals. Although some success in refining and focusing that distribution has been made[11], it remains a challenge to produce a polymer NP with great enough affinity to provide a sufficient and consistent level of function.

Recently, a small but growing body of evidence has suggested that synthetic linear polymers[12–14], dendritic polymers[15], and polymer NPs can be engineered to exhibit strong affinity for a range of target peptides[16–18], proteins[19,20] and polysaccharides[19]. Indeed, polymer NPs have been formulated with nanomolar affinity against target peptides and proteins using only combinations of hydrophobic and charged groups. These interactions mimic those arising from side chains of amino acids. However, nature also

[1]Department of Medical Biochemistry, Graduate Division of Pharmaceutical Sciences, University of Shizuoka, 52-1 Yada, Suruga-ku, Shizuoka, Shizuoka 422-8526, Japan. [2]Department of Chemistry, University of California Irvine, Irvine, California 92697, USA. [3]Department of Chemical Engineering, Kyushu University, 744 Motooka, Fukuoka 819-0395, Japan. *e-mail: oku@u-shizuoka-ken.ac.jp; miuray@chem-eng.kyushu-u.ac.jp; kjshea@uci.edu

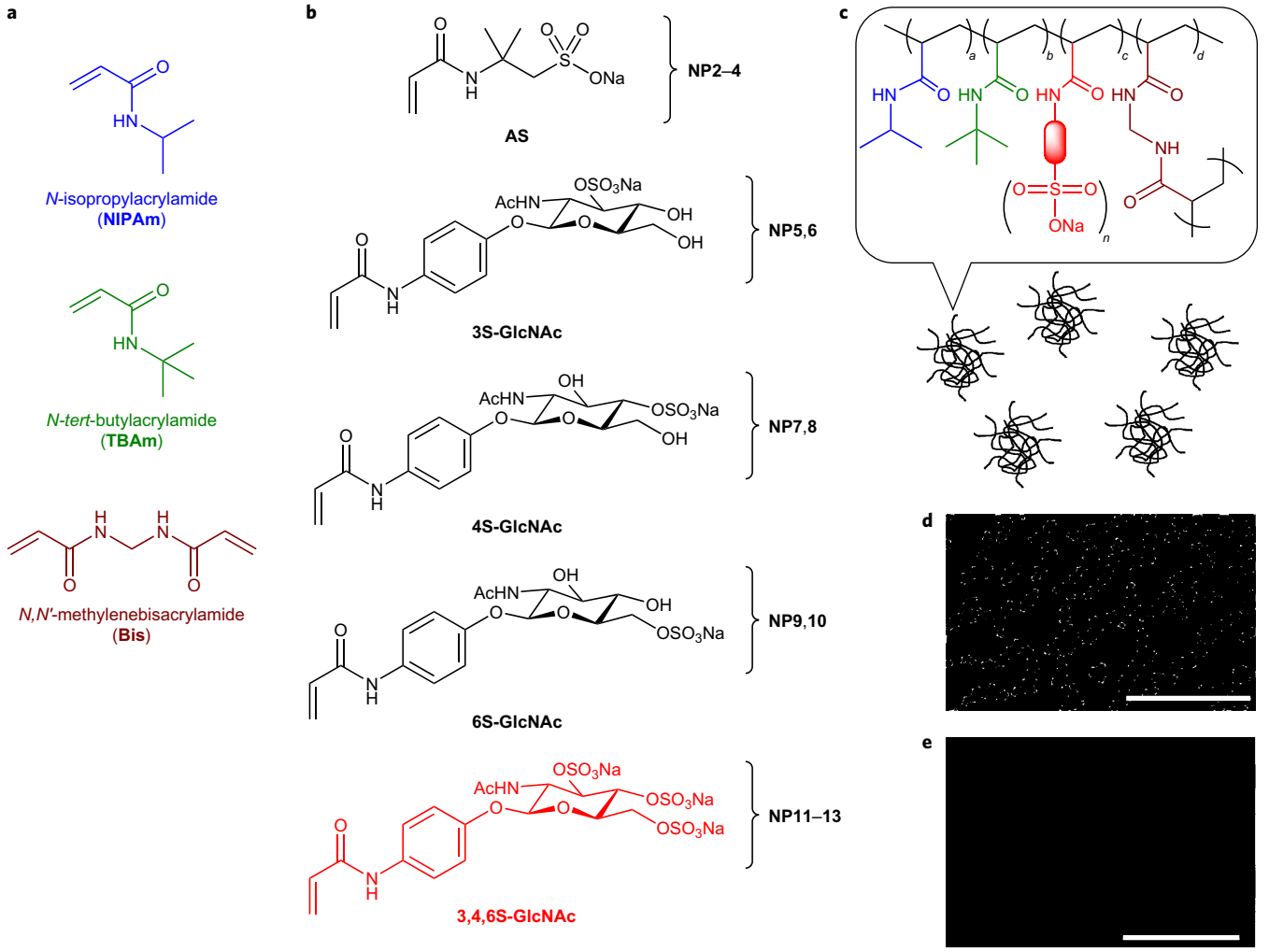

Figure 1 | The functional and sulfonate and sulfated monomers used for nanoparticle synthesis and a schematic showing the general synthesis of polymer NPs and their chemical composition. a,**b**, NPs were synthesized by free radical copolymerization of functional (**a**, NIPAm, TBAm and Bis) and anionic (**b**) monomers in the presence of SDS (0.694 mM) in water. Following the addition of ammonium persulfate (2.63 mM), the polymerization was carried out at 65 °C for 3 h. NP numbering is correlated with the functional anionic monomer used. **c**, Schematic image of polymer NPs. **d**, TEM image of **NP11**. Scale bar, 1 μm. **e**, High magnification TEM image of **NP11**. Scale bar, 100 nm.

uses other functional groups including oligosaccharides, glycosaminoglycans (GAGs), and their post-translationally modified derivatives including phosphorylated and sulfated carbohydrates and proteins to regulate biological function. Incorporation of these functional groups into a synthetic copolymer has the potential to improve affinity and/or broaden target scope. This background provides guidance for this work, the rational design of an abiotic protein affinity reagent. It should be noted, however, that affinity alone may not be sufficient to influence the function of a protein associated with maintenance of homeostasis such as a signalling protein, since inhibition of the protein's function requires masking the functional domain, as demonstrated recently[12,14]. Although a poly(styrenesulfonate) polymer stabilizes basic fibroblast growth factor (bFGF) by covalent attachment, the polymer did not inhibit the proteins activity[12,14].

Here, we describe synthesis of an abiotic hydrogel polymer NP that has been engineered with affinity for a key vascular endothelial growth factor ($VEGF_{165}$), a signalling protein that stimulates angiogenesis. $VEGF_{165}$ is a 38 kDa protein (pI 7.6) with binding-domains for its receptor (VEGFR-2) and for heparin. Heparin, a polysulfated linear polysaccharide, contains repeating disaccharide units of uronic acid and glucosamine moieties. Candidates with high affinity to $VEGF_{165}$ were identified from a screen of polymer NPs incorporating sulfonic acid, sulfated carbohydrate and hydrophobic functional monomers in a 2% crosslinked NIPAm copolymer (Fig. 1). The process, described in detail below, identified a high-affinity functional NIPAm copolymer that both binds to and inhibits the function of $VEGF_{165}$. The results establish a novel path for developing abiotic affinity reagents for functional biomacromolecules.

Results and discussion

Synthesis of sulfonated and sulfated monomers and their incorporation into polymer nanoparticles. Our strategy was to identify several domains of $VEGF_{165}$ and synthesize NPs that incorporate complementary functional monomers to interact with those domains. Although no structural information of the $VEGF_{165}$–heparin complex is available; Arg 124, 145, 149 and 159 in the $VEGF_{165}$ sequence are known to play a crucial role in heparin binding[21]. This positive charge-rich domain is spread over 40 nm^2. To target this domain, a series of polymerizable sulfonated and sulfated monomers were prepared. The monomers include 2-acrylamido-2-methylpropane sulfonic acid (AS), three positional isomers of mono-sulfated *N*-acetylglucosamines (3S-GlcNAc, 4S-GlcNAc, 6S-GlcNAc) and a tri-sulfated *N*-acetylglucosamine (3,4,6S-GlcNAc). Their structures are shown in Fig. 1b and details of their synthesis can be found in the Supplementary

Table 1 | Monomer composition, size, zeta-potential and yield of the NPs.

	NIPAm	AS	TBAm	Bis	Size (nm)	PDI	ζ potential (mV)
AS							
NP1	58	0	40	2	79.9	0.014	ND
NP2	56.3	1.7	40	2	62.7	0.120	−32.5
NP3	53	5	40	2	52.7	0.313	−32.2
NP4	48	10	40	2	62.5	0.351	−36.4
3S-GlcNAc							
NP5	56.3	1.7	40	2	86.7	0.053	−30.7
NP6	53	5	40	2	81.2	0.045	−33.8
4S-GlcNAc							
NP7	56.3	1.7	40	2	52.0	0.070	−41.0
NP8	53	5	40	2	55.0	0.145	−42.0
6S-GlcNAc							
NP9	56.3	1.7	40	2	57.1	0.066	−40.4
NP10	53	5	40	2	34.1	0.198	−34.3
3,4,6S-GlcNAc							
NP11	56.3	1.7	40	2	85.9	0.017	−38.1
NP12	53	5	40	2	87.7	0.026	−31.1
NP13	48	10	40	2	74.8	0.044	−29.7

The monomer structures can be found in Fig. 1. ND, not determined.

Information. Solutions of polymer NPs were prepared by a modified precipitation polymerization and purified by extensive dialysis (Supplementary Information). Each NP contained one of the anionic monomers, in addition to *N*-isopropylacrylamide (NIPAm), *N*-*tert*-butylacrylamide (TBAm, a hydrophobic monomer) and 2% *N*,*N*′-methylenebisacrylamide (Bis, a crosslinker) (Fig. 1a,c). Inclusion of the hydrophobic TBAm monomer was based upon crystallographic studies of the VEGF–VEGFR2 binding surface which has a number of hydrophobic amino acids that play an important role in VEGFR binding[22] and previous studies from our laboratory that established the importance of hydrophobic content of the NP for protein affinity[16,19,20,23,24]. The monomodal hydrogel particles ranged in size from 30 to 90 nm. Summaries of NP composition, particle size, ζ-potential, chemical yield and incorporation percentage of the anionic monomers (NMR analysis) are given in Table 1 and Supplementary Information (Supplementary Fig. 1). Figure 1d,e shows representative transmission electron microscopy (TEM) images of the monodisperse synthetic NPs.

Evaluation of NP affinity to $VEGF_{165}$. A quartz crystal microbalance (QCM) sensor functionalized with $VEGF_{165}$ was used to screen the NP library for protein binding. Interestingly, none of the NPs containing the negatively charged sulfonate group (AS) (**NP2–4**) showed significant binding to $VEGF_{165}$ even when the amount of AS in the NP was increased to 10% (Fig. 2a). Next, NPs containing the 3S-GlcNAc, 4S-GlcNAc or 6S-GlcNAc (mono-sulfated GlcNAc monomers, **NP5–10**), and the 3,4,6S-GlcNAc (tri-sulfated GlcNAc monomer, **NP11–13**) were screened. These NPs exhibited a wide range of $VEGF_{165}$ interaction. Among **NP5**, **7** and **9** (1.7% of mono-sulfated monomer), only **NP5** (1.7% 3S-GlcNAc) exhibited low $VEGF_{165}$ interaction (Fig. 2b).

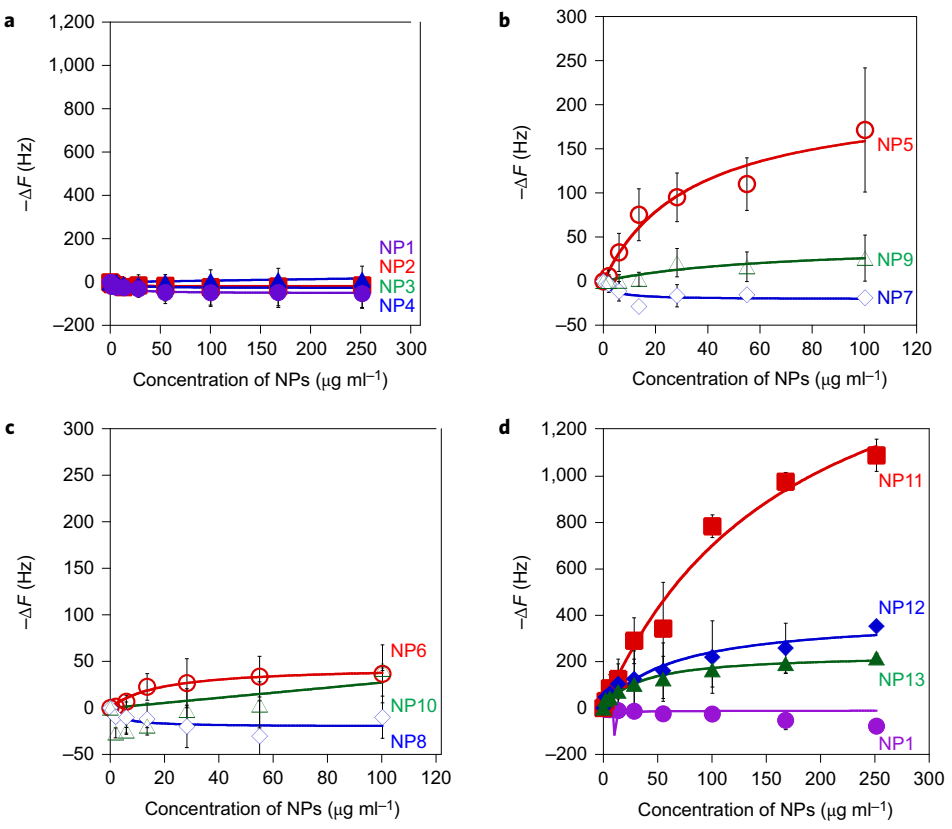

Figure 2 | Screening of polymer nanoparticles interacting with $VEGF_{165}$. a–d, QCM analysis of the $VEGF_{165}$–NP interaction. The surface of the QCM was functionalized with $VEGF_{165}$ and solutions of NPs were added to the QCM cells. **a**, $VEGF_{165}$ affinity of 0% (**NP1**), 1.7% (**NP2**), 5% (**NP3**) or 10% (**NP4**) sulfonate group containing NPs. **b**, $VEGF_{165}$ affinity of 1.7% 3S-GlcNAc (**NP5**), 4S-GlcNAc (**NP7**) or 6S-GlcNAc monomer (**NP9**) containing NPs. These NPs contain the same amount of GlcNAc monomer but one-third of a mole of the sulfate groups in **NP11** (1.7% 3,4,6S GlcNAc monomer containing NPs). **c**, $VEGF_{165}$ affinity of 5% 3S-GlcNAc (**NP6**), 4S-GlcNAc (**NP8**) or 6S-GlcNAc monomer (**NP10**) containing NPs. These NPs contain one-third of a mole of GlcNAc monomers but the same number of moles of sulfate groups as **NP11** (1.7% 3,4,6S GlcNAc monomer containing NPs). **d**, $VEGF_{165}$ affinity of 0% (**NP1**), 1.7% (**NP11**), 5% (**NP12**) or 10% (**NP13**) 3,4,6S-GlcNAc monomer containing NPs. Error bars show s.d.

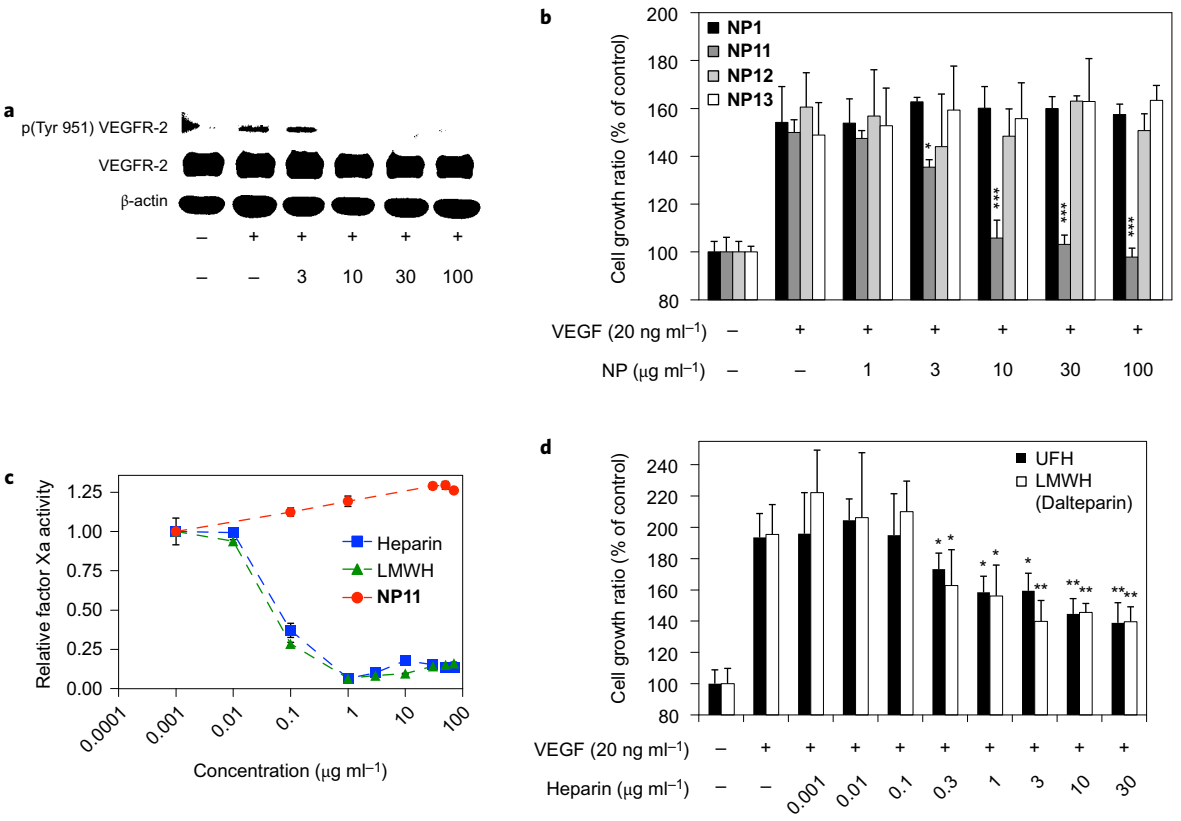

Figure 3 | *In vitro* VEGF-inhibition experiment and comparison with heparin. a, Inhibition by **NP11** of $VEGF_{165}$-dependent VEGFR-2 phosphorylation. HUVECs were cultured without growth factors and serum. Twelve hours after the medium change, cells were incubated with EBM-2 containing 20 ng ml^{-1} of $VEGF_{165}$ and different concentrations of NPs for 2 h at 37 °C. Then, phosphorylated [Tyr 951] VEGFR-2 was detected by western blotting. **b**, Inhibition of $VEGF_{165}$-dependent cell growth by **NP1** and **NP11–NP13**. HUVECs were cultured without growth factors and serum. Twelve hours after the medium change, the cells were treated with NPs and $VEGF_{165}$ (20 ng ml^{-1}) for 48 h. Then, viable cells were determined by MTT assay. Significant differences: $^{*}P < 0.05$ and $^{***}P < 0.001$ versus 0 μg ml^{-1}. Error bars show s.d. **c**, Factor Xa (FXa) binding study to AT III. After incubation of AT III with several concentrations of **NP11**, UFH or LMWH (Dalteparin), FXa was added. Then, the remaining FXa was measured. **d**, Inhibition of $VEGF_{165}$-dependent cell growth heparin with (UFH or LMWH (dalteparin)). HUVECs were cultured without growth factors and serum. Twelve hours after the medium change, the cells were treated with several concentrations of heparins and $VEGF_{165}$ (20 ng ml^{-1}) for 48 h. Then, viable cells were determined by MTT assay. Significant differences: $^{*}P < 0.05$ and $^{***}P < 0.001$ versus 0 μg ml^{-1} . Error bars show s.d. *P* values were calculated by ANOVA with the Tukey post hoc test.

NP6, **8** and **10** (5% of these same mono-sulfated monomers) showed much lower interaction with the protein (Fig. 2c). Collectively, the results establish that NP binding to $VEGF_{165}$ is dependent on the nature of the charged group (sulfate versus sulfonate), the GlcNAc scaffold and the position of sulfation (3′ versus 4′ or 6′). The sensitivity to the positional isomers on the carbohydrate skeleton may not be surprising as there are a number of studies that report the importance of sulfate position on affinity to target proteins. For example, the 3-*O*-sulfo group within heparin has been reported to be essential for binding to antithorombin III[25], the fibroblast growth factor 7 (FGF-7)[26] and the 6-*O*-sulfo groups for binding to FGF-1 (ref. 27).

The screen of **NP11–13** incorporating the 3,4,6S-GlcNAc monomer showed far more dramatic results. Although the particle size and ζ-potential of **NP11–13** were not significantly different from other NPs tested (Table 1), **NP11** strongly interacted with $VEGF_{165}$ (Fig. 2d). The observed frequency change (up to 1,200 Hz) was six times higher than that of **NP5**. A control study confirmed that the NPs in this study do not interact with the blocking agent (bovine serum albumin, BSA) (Supplementary Fig. 2a). **NP11** affinity is estimated to be ~380 nM (QCM) (Supplementary Fig. 2b). This result suggests that small local clusters of negative charge from the 3,4,6S-GlcNAc monomer are important for NP binding to $VEGF_{165}$. The significance of hydrophobic groups (TBAm) was established by observing that decreasing the TBAm content of NPs containing 1.7% of the 3,4,6 tri-sulfated GlcNAc monomer from 40% (**NP11**) to 20% (**NP14**) to 0% (**NP15**) significantly reduced and eventually eliminated the interaction with $VEGF_{165}$ (Supplementary Fig. 3), suggesting that in addition to localized multipoint electrostatic interactions, hydrophobic content is an essential component for the **NP11**–$VEGF_{165}$ interaction.

An experiment was designed to evaluate if **NP11** inhibits binding of $VEGF_{165}$ to the VEGFR-2 by binding selectively to VEGFR-2. In screens, **NP11** was found to have only modest affinity to VEGFR-2 (Supplementary Fig. 5), saturating at a concentration of ~250 μg ml^{-1}. The subsequent $VEGF_{165}$ binding inhibition assay therefore, was run at a NP concentration of 50 μg ml^{-1}. $VEGF_{165}$ showed high affinity for VEGFR-2, whereas $VEGF_{165}$ did not bind to VEGFR-2 in **NP11** containing solutions. The result indicates that **NP11** does not inhibit the $VEGF_{165}$–VEGFR-2 interaction by binding to the receptor but by sequestering $VEGF_{165}$ in solution before it binds to the receptor.

As stated previously, Arg 124, 145, 149 and 159 in the $VEGF_{165}$ sequence are known to play a crucial role in heparin binding23. We speculate that NPs incorporating clusters of negative charge, such as the multiply sulfated 3,4,6S-GlcNAc group, are effective at binding to this positively charged domain of $VEGF_{165}$. Validation that a significant component of the interaction between $VEGF_{165}$ and **NP11** is at the heparin-binding domain comes from QCM studies with $VEGF_{121}$, a truncated growth factor that lacks the heparin-

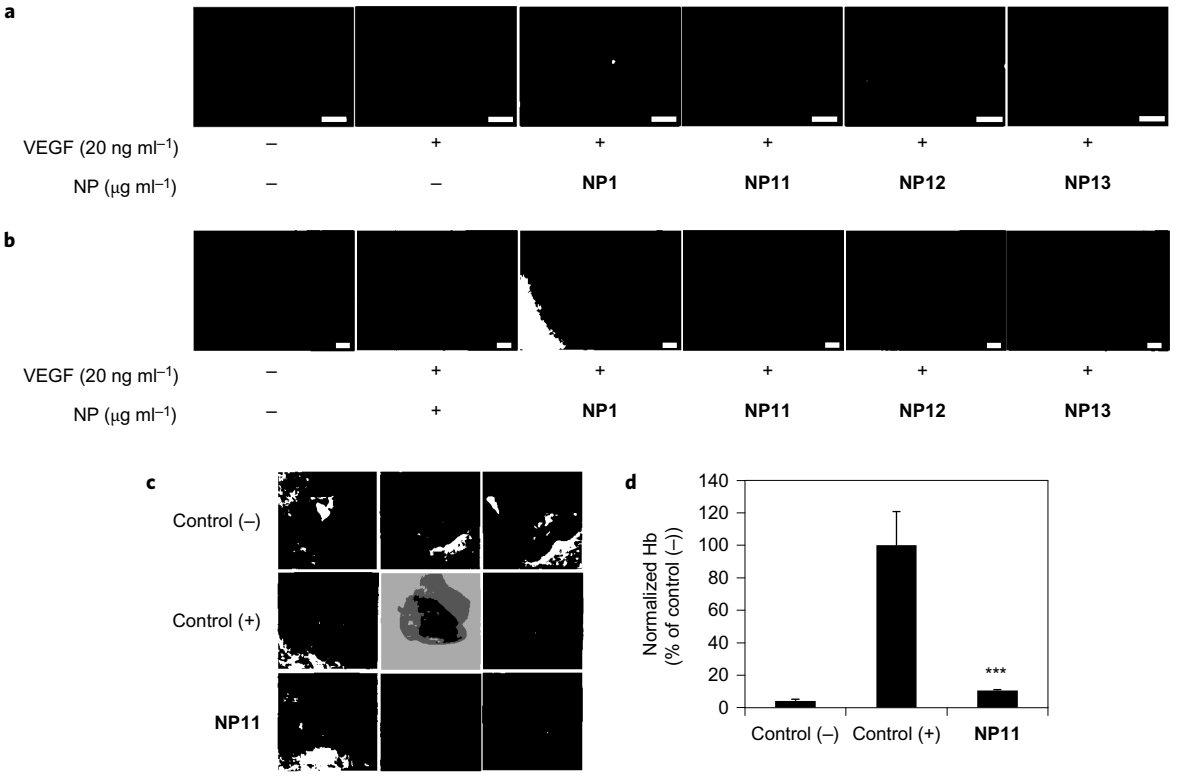

Figure 4 | Anti-angiogenic effect of NPs. a, Inhibition of $VEGF_{165}$-dependent cell motility by **NP1** and **NP11–NP13**. Fluorescently labelled HUVECs were seeded onto Matrigel coated FluoroBlok insert. $VEGF_{165}$ (20 ng ml^{-1}) was added to the cells with or without **NPs** (30 μg ml^{-1}). The inserts were incubated for 24 h at 37 °C. Then, the cells that invaded to the lower side of the membrane were observed. Scale bars, 30 μm. **b**, Inhibition of $VEGF_{165}$-dependen capillary tube formation in the presence of **NP1** and **NP11–NP13**. $VEGF_{165}$ (20 ng ml^{-1}) and/or NPs (30 μg ml^{-1}) were added to HUVECs and incubated for 12 h at 37 °C. Scale bars, 30 μm. **c**, Inhibition of *in vivo* angiogenesis in Matrigel plugs implanted in mice. BALB/c-male mice were subcutaneously injected with a liquid Matrigel (6 mg ml^{-1}). Matrigel contained 20 nM mouse $VEGF_{165}$ and 42 units of heparin, and **NP11** at a final concentration of 300 μg ml^{-1} . Matrigel and PBS or mouse $VEGF_{165}$ and heparin were injected as negative and positive controls, respectively. Plugs were removed from mice and photographed after 10 days. **d**, Haemoglobin (Hb) content within Matrigel plugs was quantified and depicted as a percentage of Hb. Significant differences: ***$P < 0.001$ versus control (+). Error bars show s.d. *P* values were calculated by ANOVA with the Tukey post hoc test.

binding domain. **NP11** shows little affinity for this protein (Supplementary Fig. 4). This result coupled with the TBAm results point to the importance of cooperative interactions to realize NP-protein affinity.

That the clustered charge of the tri-anionic monomer may also contribute to the NP–protein affinity comes from comparison with NPs containing an equivalent amount of charged groups using singly charged monomers. These NPs would be less likely to create a 'cluster' of negative charge due to electrostatic repulsion of the negative charges in the polymerization step. The constrained triply charged monomer does not suffer from this effect. So, although the net charge of 5% mono-sulfate NPs (**NP6**, **8** and **10**) and 1.7% 3,4,6S NPs (**NP11**) is the same, we suggest that the local presentation of charge in the NPs is significantly different and is a contributing factor to the difference in affinity. We note however that these trends are not expected to manifest themselves in ζ-potential measurements. A decrease of ζ-potential with an increase of surface charge density has been observed previously and explained by an ion condensation model. It was predicted theoretically and shown experimentally that for a sufficiently high surface charge density, nearby counter ions can collapse on the particle or polyelectrolyte lowering the effective magnitude of the particle ζ-potential[28–32].

Interestingly, both **NP12** and **NP13** containing a higher percentage of trisulfate monomer 3,4,6S-GlcNAc (5 or 10%) had substantially lower protein interaction compared with **NP11**. This would appear to be a consequence of the complexity of protein surfaces and the sensitivity to the exact (average) composition of the affinity reagent. In addition to the heparin-binding domain, $VEGF_{165}$ has a number of negatively charged amino acids on its surface. The diminished interaction for $VEGF_{165}$ of **NP12** (5%, 3,4,6S-GlcNAc) compared with **NP11** (1.7% 3,4,6S-GlcNAc) reflects a required balance of electrostatic interactions between the protein surface and the NP; a higher loading of the tri-anionic 3,4,6S-GlcNAc eventually results in repulsion between the protein and NP. This sensitivity to both charge and hydrophobic contributions calls attention to the uniqueness of each protein (and NP) domain, an attribute that is responsible in part for the selectivity of protein–protein binding in signal transduction and related phenomena.

***In vitro* VEGF-inhibition experiments and comparison with heparin.** Binding of $VEGF_{165}$ to VEGFR-2, its native receptor, is known to induce the phosphorylation of VEGFR-2 and trigger downstream cell signalling events[33]. Although there is no direct evidence for the interaction of **NP11** with the VEGFR-2 binding domain of $VEGF_{165}$, we speculate that binding of this relatively large multifunctional NP (~85 nm) with the protein (<10 nm), could antagonize binding to VEGFR-2. An *in vitro* study was carried out to confirm the inhibitory effect of **NP11** on $VEGF_{165}$-induced phosphorylation of VEGFR-2. Human umbilical vein endothelial cells (HUVEC) were incubated with the $VEGF_{165}$ at several concentrations of NPs. **NP11** strongly inhibited the phosphorylation (Tyr 951) at a concentration of 10 μg ml^{-1} (Fig. 3a), whereas **NP1**, **NP12** and **NP13** did not inhibit the phosphorylation of VEGFR-2 at 100 μg ml^{-1} (Supplementary

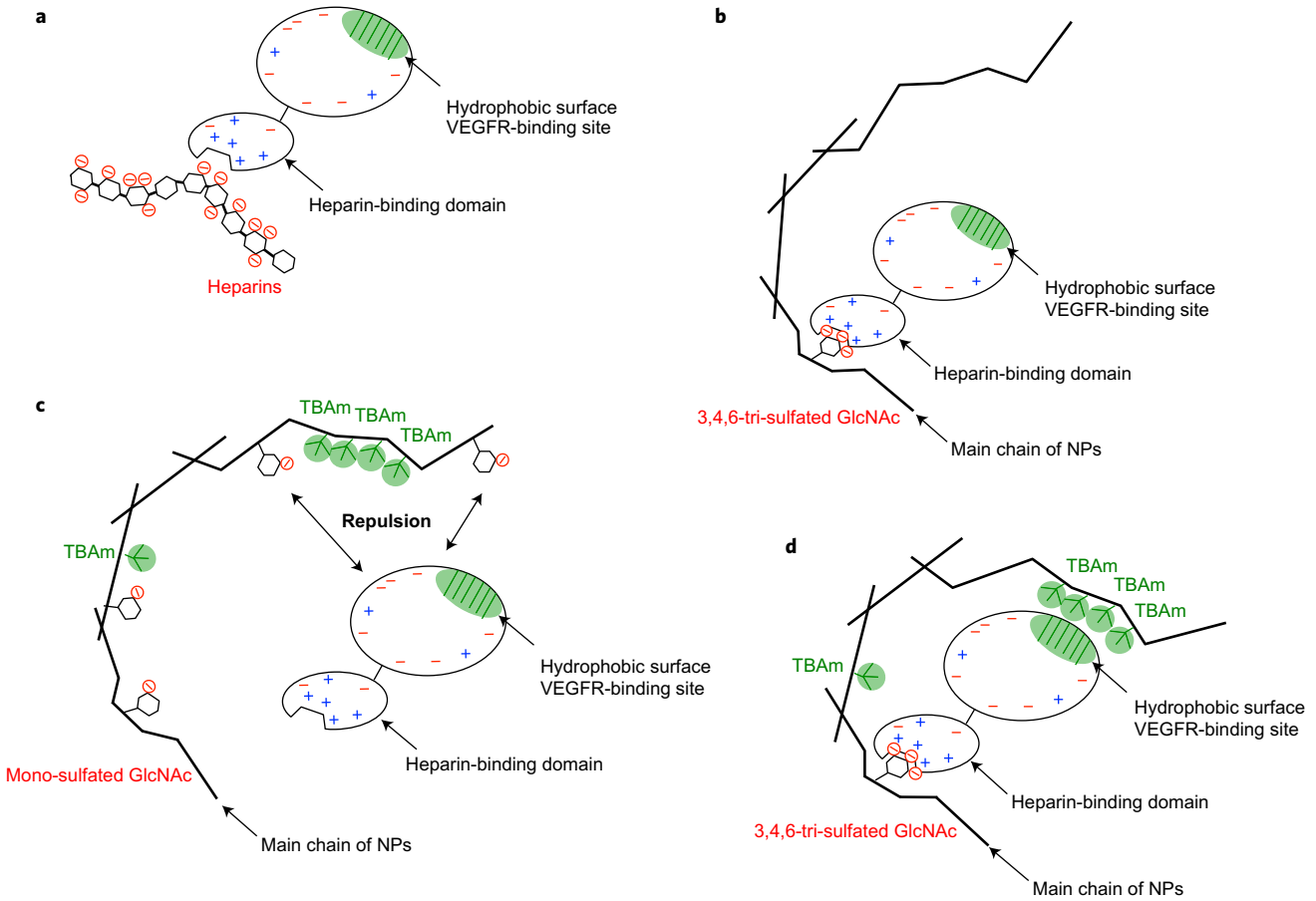

Figure 5 | Schematic images of the interaction of heparins and $VEGF_{165}$ with NPs of various compositions. a, Heparin and $VEGF_{165}$ interaction. Heparin binds to the heparin-binding domain of $VEGF_{165}$. **b**, $VEGF_{165}$ interaction with NPs that lack TBAm, a hydrophobic monomer (**NP15**). Only **NP15** with 3,4,6S-GlcNAc binds to the heparin-binding domain of $VEGF_{165}$. **c**, $VEGF_{165}$ interaction with NPs containing TBAm and 5% mono-sulfated GlcNAc monomer (**NP10**). Slightly higher concentrations of randomly distributed sulfate groups in the NP induce electrostatic repulsion to $VEGF_{165}$. Localized multiple negative charges play an important role in NP binding to $VEGF_{165}$. **d**, $VEGF_{165}$ interaction with **NP11** containing TBAm and 1.7% 3,4,6 tri-sulfated monomer. 3,4,6S-GlcNAc interacts with the heparin-binding domain of $VEGF_{165}$ and TBAm interacts with hydrophobic rich receptor binding domain of $VEGF_{165}$. Both charge and hydrophobic contributions contribute to the affinity between $VEGF_{165}$ and **NP11**.

Fig. 5a–c). We conclude that **NP11** inhibits VEGFR-2 phosphorylation by sequestering $VEGF_{165}$. Phosphorylation of VEGFR-2 is the signalling event for endothelial cell growth. To evaluate the influence of NPs on $VEGF_{165}$-dependent cell growth, $VEGF_{165}$ and NPs were added to HUVECs. **NP11** dose-dependently inhibited $VEGF_{165}$-dependent cell growth, a result that correlates with the phosphorylation inhibition results (Fig. 3b). Indeed, the half maximal inhibitory concentration (IC_{50}) of $VEGF_{165}$-dependent HUVEC growth by **NP11** was approximately 5 μg ml^{-1}. At a concentration of 10 μg ml^{-1}, the growth rate was approximately equal to that of control cells without $VEGF_{165}$ (Fig. 3b). These results establish that 10 μg ml^{-1} of **NP11** effectively inhibits $VEGF_{165}$-dependent phosphorylation and subsequent downstream cell proliferation. Importantly, **NP11** was not taken up into nor did it bind HUVECs even when the NP concentration was increased to 300 μg ml^{-1} (Supplementary Fig. 6).

Unfractionated heparin (UFH) and low-molecular-weight heparin (LMWH, dalteparin) also bind to $VEGF_{165}$. However, these sulfated carbohydrates bind to a number of functional proteins and produce a number of off-target outcomes, perhaps the most important of which is their anti-coagulant activity. For example, following binding of heparin to antithrombin III (AT III), factor Xa (FXa), a key enzyme in the blood coagulation cascade, binds to the complex and induces anti-coagulation. Since **NP11** has affinity to the heparin-binding domain of $VEGF_{165}$ it is important to establish if the NP exhibits other heparin-like properties. Significantly, we found that **NP11** does not inhibit the activity of FXa (Fig. 3c). In addition, QCM analysis indicates that **NP11** and AT III interaction was weak compared with **NP11** and $VEGF_{165}$ interaction (Supplementary Fig. 7a). On the other hand, the function of FXa was inhibited by heparins. Even at a concentration of 100 μg ml^{-1}, **NP11** exhibited no inhibition of FXa. The observation suggests that although **NP11** selectively inhibits $VEGF_{165}$-dependent activity by multiple interactions with both heparin and VEGFR binding domains, it does not interfere with the coagulation cascade. These same studies also allowed us to establish that **NP11** did not exhibit cytotoxicity in the range of 0–100 μg ml^{-1} (Supplementary Fig. 7b). Since there is little homology in heparin binding domains[34], these results suggest a potential path to selective abiotic affinity reagents for proteins with heparin-binding domains or heparin-mediated processes. We are currently evaluating this potential.

UFH or LMWH also showed a dose-dependent inhibition of $VEGF_{165}$-dependent HUVEC growth (Fig. 3d) with IC_{50} of 1 and 0.3 μg ml^{-1} for UFH and LMWH, respectively. However, in contrast to **NP11**, at those concentrations both UFH and LMWH strongly inhibit FXa, and interfere with the clotting cascade, which would result in undesired side effects upon administration (Fig. 3c)[13,35]. These results establish that **NP11** is not a heparin mimic and does not exhibit an important heparin function. Its action cannot be replaced by heparin or its derivatives.

Anti-angiogenic effect of the NPs. $VEGF_{165}$ is known to play a major role in angiogenesis and is a critical factor during the early stages of tumour growth[36–38]. In angiogenesis, endothelial cell migration and invasion into the extracellular matrix are important steps in the production of angiogenic blood vessels. The effect of **NP11** on downstream angiogenic activity was evaluated by experiments that revealed only **NP11** (30 μg ml^{-1}) significantly inhibits $VEGF_{165}$-induced HUVECs migration and invasion (Fig. 4a; Supplementary Fig. 8a–c). In addition, tube formation by endothelial cells is the first step in formation of angiogenic blood vessels. HUVECs were seeded onto a Matrigel-coated plate and then $VEGF_{165}$ (20 ng ml^{-1}) and NPs (30 μg ml^{-1}) were added to the medium. HUVECs formed capillary-like structures only upon addition of $VEGF_{165}$. However, the addition of **NP11** effectively inhibits the $VEGF_{165}$-induced capillary tube formation (Fig. 4b; Supplementary Fig. 9). On the other hand, capillary tube formation was not inhibited by NPs with less pronounced $VEGF_{165}$ affinity such as **NP1**, **NP12** and **NP13**. The inhibition of downstream anti-angiogenic function is a consequence of the sequestration of $VEGF_{165}$ by **NP11**.

To evaluate the efficacy of **NP11** in blocking new blood vessel formation under more challenging conditions, a Matrigel plug assay was performed. Mice were subcutaneously injected with Matrigel alone (negative control); $VEGF_{165}$ and heparin (positive control); or $VEGF_{165}$, heparin and **NP11**. Ten days after the implantation, Matrigel plugs were removed and the haemoglobin content was measured. As shown in Fig. 4c, incorporation of **NP11** into the Matrigel plug effectively inhibited blood vessel formation. Indeed, the haemoglobin content in the Matrigel plug was very close to that of the negative control (absence of $VEGF_{165}$, Fig. 4d). Collectively, these results establish the ability of **NP11** to inhibit recruitment of endothelial cells and prevent new blood vessel formation by sequestrating $VEGF_{165}$.

Conclusions

In this report, we describe a process for synthesizing an abiotic protein affinity reagent. Polymer NPs with affinity for $VEGF_{165}$, a key vascular endothelial growth factor, were identified from a screen of a small library of NPs prepared by copolymerizing monomers with functionality complementary to the heparin and VEGFR-2 binding domains of the protein. Polymer NPs with nanomolar affinity to $VEGF_{165}$ were realized by incorporating 1.7% of a trisulfated *N*-acetylglucosamine (3,4,6S-GlcNAc) monomer, a hydrophobic group, *N-tert*-butylacrylamide (TBAm), in a 2% crosslinked NIPAm copolymer. NP affinity was 'tuned' by varying the amount of both 3,4,6S-GlcNAc and TBAm monomer incorporation since increasing the 3,4,6S-GlcNAc monomer and/or decreasing the hydrophobic monomer (TBAm) content decreased affinity to the protein. The NP–protein interaction was designed to take place over multiple protein domains (Fig. 5), a factor that was validated by compositional variation of the NP and by screening NP affinity against truncated proteins. The optimized NP (**NP11**) was shown to inhibit $VEGF_{165}$-dependent growth, tube formation, migration and invasion of HUVECs *in vitro* through suppression of VEGFR-2 phosphorylation. Importantly, at concentrations needed to inhibit VEGFR-2 phosphorylation, the optimized NP (**NP11**), did not inhibit the activity of FXa. This result distinguishes the NP from heparin and its derivatives both of which inhibit VEGF-dependent HUVEC growth in addition to enzymes involved in the blood coagulation cascade. **NP11** was also shown to inhibit $VEGF_{165}$-dependent angiogenesis in a Matrigel plug in the body of living mice. These results establish that NPs can be engineered to bind to and interfere with a signalling protein ($VEGF_{165}$), by targeting specific domains of the protein by inclusion of both hydrophobic and a novel trisulfated carbohydrate functional group into a 2% crosslinked NIPAm synthetic polymer. The carbohydrate platform permits the stereocontrolled incorporation of clusters of functional groups, a feature not available from amino acid side chains. These results establish the potential for realizing abiotic protein affinity reagents with many of the functions of more traditional protein affinity reagents.

Methods

For further details, see Supplementary Information.

Preparation of NPs. NPs were synthesized by free-radical copolymerization of *N*-isopropylacrylamide (NIPAm) crosslinked with 2 mol% *N*,*N*′-methylenebisacrylamide (bis). *N-tert*-butylacrylamide (TBAm) and 3-sulfo-*N*-acetylglucosamines (3S), 4-sulfo-*N*-acetylglucosamines (4S), 6-sulfo-*N*-acetylglucosamines (6S) or 3,4,6-sulfo-*N*-acetylglucosamines (3,4,6S) were used as hydrophobic and negatively charged functional monomers. The polymerization was carried out at 65 °C for 3 h under a nitrogen atmosphere. The polymerized solutions were purified by dialysis (Supplementary Text).

Characterization of NPs. The hydrodynamic diameter of NPs was determined in aqueous solution by dynamic light scattering (Zetasizer Nano ZS) (Supplementary Text).

Quantification of GlcNAc monomers in NPs by ^{1}H-NMR. In order to determine the ratio of TBAm, NIPAm and GlcNAc in the polymer, ^{1}H-NMR spectroscopy was utilized using an acquisition time of 30 s (Supplementary Text and Supplementary Figs 10–19).

Quartz crystal microbalance analysis. An Affinix Q4 quartz crystal microbalance (QCM) instrument (ULVAC, Kanagawa, Japan) was used to quantify interactions between the NPs and proteins (Supplementary Text).

Cell culture. Human umbilical vein endothelial cells (HUVECs, Takara Bio, Otsu, Shiga, Japan) were maintained in endothelial growth medium-2 (EGM-2, Cambrex Corporation, Walkersville, USA) at 37 °C under 5% CO_2 in a humidified chamber (Supplementary Text).

Cell proliferation and cytotoxicity assay. HUVECs were treated with NPs and $VEGF_{165}$ (20 ng ml^{-1}) for 48 h. Then, Tetracolor ONE (Seikagaku, Tokyo, Japan) was added to each well in accordance with the manufacturer's instructions. The amount of formazan was measured with a Tecan Infinite M200 micro plate reader at a test wavelength of 450 nm and a reference wavelength of 630 nm (Supplementary Text).

Western blotting. HUVECs were incubated in EBM-2 containing 20 ng ml^{-1} of $VEGF_{165}$ and several concentrations of NPs for 2 h at 37 °C. The cells were then lysed. The cell extracts were subjected to 7.5% SDS–PAGE and transferred electrophoretically to polyvinylidene difluoride (PVDF) membranes (Millipore, Billerica, USA). The membranes were incubated with a primary antibody (against β-actin, VEGF receptor-2 or pVEGF receptor-2 [Tyr 951]) for 24 h at 4 °C. Then, they were incubated for 1 h at room temperature with HRP-conjugated secondary antibody. Each sample was developed using a chemiluminescent substrate (ECL; GE Healthcare Bioscience), and each protein was detected with the LAS-3000 mini system (Supplementary Text).

Motility and invasion assays. Motility and invasion assays were performed using a modification of a previously described method (Supplementary Text).

Capillary tube formation assay. HUVECs were seeded onto Matrigel coated plates. Then, $VEGF_{165}$ (20 ng ml^{-1}) and/or NPs (30 μg ml^{-1}) were added to the HUVECs and were incubated for 12 h at 37 °C. Photographs were taken with an Olympus IX71 microscope (Supplementary Text).

Statistical analysis. Differences between groups were evaluated by an analysis of variance (ANOVA) with the Tukey post hoc test.

Received 10 April 2015; accepted 15 December 2016; published online 27 March 2017

References

1. Hardiman, G. Next-generation antibody discovery platforms. *Proc. Natl Acad. Sci. USA* **109,** 18245–18246 (2012).
2. Dubel, S., Stoevesandt, O., Taussig, M. J. & Hust, M. Generating recombinant antibodies to the complete human proteome. *Trends Biotechnol.* **28,** 333–339 (2010).
3. Lollo, B., Steele, F. & Gold, L. Beyond antibodies: new affinity reagents to unlock the proteome. *Proteomics* **14,** 638–644 (2014).

4. Cobaugh, C. W., Almagro, J. C., Pogson, M., Iverson, B. & Georgiou, G. Synthetic antibody libraries focused towards peptide ligands. *J. Mol. Biol.* **378,** 622–633 (2008).
5. Marx, V. Calling the next generation of affinity reagents. *Nat. Methods* **10,** 829–833 (2013).
6. Arkin, M. R. & Wells, J. A. Small-molecule inhibitors of protein–protein interactions progressing towards the dream. *Nat. Rev. Drug Discov.* **3,** 301–317 (2004).
7. Klinger, D. & Landfester, K. Stimuli-responsive microgels for the loading and release of functional compounds fundamental concepts and applications. *Polymer* **53,** 5209–5231 (2012).
8. Schild, H. G. Poly(*N*-isopropylacrylamide): experiment, theory and application. *Prog. Polym. Sci.* **17,** 163–249 (1992).
9. Uversky, V. N., Oldfield, C. J. & Dunker, A. K. Intrinsically disordered proteins in human diseases: introducing the D^2 concept. *Annu. Rev. Biophys.* **37,** 215–246 (2008).
10. Rogers, J. M., Wong, C. T. & Clarke, J. Coupled folding and binding of the disordered protein PUMA does not require particular residual structure. *J. Am. Chem. Soc.* **136,** 5197–5200 (2014).
11. Hoshino, Y. *et al.* Affinity purification of multifunctional polymer nanoparticles. *J. Am. Chem. Soc.* **132,** 13648–13650 (2010).
12. Christman, K. L. *et al.* Nanoscale growth factor patterns by immobilization on a heparin-mimicking polymer. *J. Am. Chem. Soc.* **130,** 16585–16591 (2008).
13. Oh, Y. I., Sheng, G. J., Chang, S. K. & Hsieh-Wilson, L. C. Tailored glycopolymers as anticoagulant heparin mimetics. *Angew. Chem. Int. Ed.* **52,** 11796–11799 (2013).
14. Nguyen, T. H. *et al.* A heparin-mimicking polymer conjugate stabilizes basic fibroblast growth factor. *Nat. Chem.* **5,** 221–227 (2013).
15. Dernedde, J. *et al.* Dendritic polyglycerol sulfates as multivalent inhibitors of inflammation. *Proc. Natl Acad. Sci. USA* **107,** 19679–19684 (2010).
16. Hoshino, Y. *et al.* The rational design of a synthetic polymer nanoparticle that neutralizes a toxic peptide *in vivo*. *Proc. Natl Acad. Sci. USA* **109,** 33–38 (2012).
17. Yoshimatsu, K., Koide, H., Hoshino, Y. & Shea, K. J. Preparation of abiotic polymer nanoparticles for sequestration and neutralization of a target peptide toxin. *Nat. Protoc.* **10,** 595–604 (2015).
18. Koch, S. J., Renner, C., Xie, X. L. & Schrader, T. Tuning linear copolymers into protein-specific hosts. *Angew. Chem. Int. Ed.* **45,** 6352–6355 (2006).
19. Lee, S. H. *et al.* Engineered synthetic polymer nanoparticles as IgG affinity ligands. *J. Am. Chem. Soc.* **134,** 15765–15772 (2012).
20. Yoshimatsu, K. *et al.* Temperature-responsive "catch and release" of proteins by using multifunctional polymer-based nanoparticles. *Angew. Chem. Int. Ed.* **51,** 2405–2408 (2012).
21. Robinson, C. J., Mulloy, B., Gallagher, J. T. & Stringer, S. E. $VEGF_{165}$-binding sites within heparan sulfate encompass two highly sulfated domains and can be liberated by K5 lyase. *J. Biol. Chem.* **281,** 1731–1740 (2006).
22. Brozzo, M. S. *et al.* Thermodynamic and structural description of allosterically regulated VEGFR-2 dimerization. *Blood* **119,** 1781–1788 (2012).
23. Hoshino, Y. *et al.* Design of synthetic polymer nanoparticles that capture and neutralize a toxic peptide. *Small* **5,** 1562–1568 (2009).
24. Hoshino, Y. *et al.* Recognition, neutralization, and clearance of target peptides in the bloodstream of living mice by molecularly imprinted polymer nanoparticles a plastic antibody. *J. Am. Chem. Soc.* **132,** 6644–6645 (2010).
25. Richard, B., Swanson, R. & Olson, S. T. The signature 3-*O*-sulfo group of the anticoagulant heparin sequence is critical for heparin binding to antithrombin but is not required for allosteric activation. *J. Biol. Chem.* **284,** 27054–27064 (2009).
26. Ye, S. *et al.* Structural basis for interaction of FGF-1, FGF-2, and FGF-7 with different heparan sulfate motifs. *Biochemistry* **40,** 14429–14439 (2001).
27. Guimond, S., Maccarana, M., Olwin, B. B., Lindahl, U. & Rapraeger, A. C. Activating and inhibitory heparin sequences for FGF-2 (basic FGF). Distinct requirements for FGF-1, FGF-2, and FGF-4. *J. Biol. Chem.* **268,** 23906–23914 (1993).
28. Manning, G. S. Counterion binding in polyelectrolyte theory. *Acc. Chem. Res.* **12,** 443–449 (1979).
29. Quesada-Perez, M., Callejas-Fernandez, J. & Hidalgo-Alvarez, R. An experimental test of the ion condensation theory for spherical colloidal particles. *J. Colloid Interface Sci.* **233,** 280–285 (2001).
30. Manning, G. S. The critical onset of counterion condensation: A survey of its experimental and theoretical basis. *Ber. Bunsen. Phys. Chem.* **100,** 909–922 (1996).
31. Popov, A. & Hoagland, D. A. Electrophoretic evidence for a new type of counterion condensation. *J. Polym. Sci. Pol. Phys.* **42,** 3616–3627 (2004).
32. Manning, G. S. Counterion condensation on charged spheres, cylinders, and planes. *J. Phys. Chem. B* **111,** 8554–8559 (2007).
33. Graells, J. *et al.* Overproduction of VEGF165 concomitantly expressed with its receptors promotes growth and survival of melanoma cells through MAPK and PI3K signaling. *J. Invest. Dermatol.* **123,** 1151–1161 (2004).
34. Munoz, E. M. & Linhardt, R. J. Heparin-binding domains in vascular biology. *Arterioscl. Throm. Vas.* **24,** 1549–1557 (2004).
35. Warkentin, T. E. *et al.* Heparin-induced thrombocytopenia in patients treated with low-molecular-weight heparin or unfractionated heparin. *N. Engl. J. Med.* **332,** 1330–1336 (1995).
36. Karamysheva, A. F. Mechanisms of angiogenesis. *Biochemistry (Mosc.)* **73,** 751–762 (2008).
37. Carmeliet, P. & Jain, R. K. Angiogenesis in cancer and other diseases. *Nature* **407,** 249–257 (2000).
38. Brekken, R. A. *et al.* Selective inhibition of vascular endothelial growth factor (VEGF) receptor 2 (KDR/Flk-1) activity by a monoclonal anti-VEGF antibody blocks tumor growth in mice. *Cancer Res.* **60,** 5117–5124 (2000).

Acknowledgements

Financial support from the University of California Cancer Research Coordinating Committee and the National Science Foundation (DMR-1308363) is gratefully acknowledged. This research was also supported by a Grant-in-Aid for JSPS Postdoctoral Fellowships for Research Abroad (25-426), Grant-in-Aid for MEXT (23111716 and 25107726), Grant-in-Aid for Young Scientists (A) (23685027), The Kurata Memorial Hitachi Science and Technology Foundation and The Uehara Memorial Foundation. We thank T. Ozeki for help with QCM measurements.

Author contributions

H.K., K.Y., K.J.S., Y.H., N.O. and Y.M. designed the research and H.K. and Y.H. designed the experiments. Y.H., Y.N., and Y.M. synthesized GlcNAc monomers. H.K, K.Y., A.W., S.-H.L. and Y.Y. performed the binding assay with QCM and synthesized NPs. Y.N. took TEM pictures of the NPs. H.K., A.O. and S.A. preformed the *in vitro* assay with supervision from N.O.; H.K., K.Y., Y.M., Y.H., N.O. and K.J.S. wrote the manuscript. All authors discussed the results and commented on the manuscript.

Additional information

Supplementary information is available in the online version of the paper. Reprints and permissions information is available online at www.nature.com/reprints. Correspondence and requests for materials should be addressed to N.O., Y.M. and K.J.S.

Competing financial interests

The authors declare no competing financial interests.